First principles theories and MgB_2 at ambient and high pressures*

B. K. Godwal†, P. Modak, A. K. Verma, D. M. Gaitonde and R. S. Rao
High Pressure Physics Division, Bhabha Atomic Research Centre, Mumbai 400 085, India

MgB_2, the recently discovered high temperature superconductor, is considered from the perspective of first principles electronic structure and phonon calculations. The discrepancies in the estimated quantities related to its superconductivity *vis-à-vis* their experimental values, and reasons thereof are discussed. We predict hole-doped light-atom compound MgB_2C_2 to be a strong candidate for high temperature superconductivity. Anomalous high pressure behaviour seen in MgB_2 near 18 GPa is discussed, and we have demonstrated for the first time by calculating the high pressure electronic structure with frozen-in phonon-mode displacement of atoms, that phonon-assisted electronic topological transition is the probable cause of the anomaly.

THE discovery of superconductivity[1] with remarkably high transition temperature in the binary compound MgB_2, with $T_c \sim 39$ K has initiated extensive studies of this compound. At ambient conditions, MgB_2 crystallizes in the layered hexagonal AlB_2 type structure, where B atoms form a primitive honeycomb lattice consisting of graphite-like sheets separated by hexagonal layers of Mg atoms. Boron isotope effect[2] has been observed in MgB_2 giving credence to the belief that the pairing mechanism leading to superconductivity is of phononic origin. On substituting Al for Mg it is found[3] that T_c decreases. Another intriguing feature of this compound is that spectroscopies, which probe the superconducting gap, have reported conflicting results. Thus some measurements have seen[4,5] a single gap, whereas others[6,7] have measured two different gaps. The inplane penetration depth in this compound is measured[8] to be ~1000 Å whereas the coherence length is found[9] to be 70 Å.

A natural question that arises is whether studies of the electronic band structure of this material combined with BCS theory or its strong coupling variant can account for the superconducting state properties of this compound. As the active electrons at the Fermi energy are primarily *s* and *p* electrons from the boron atoms it seems likely that unlike in the case of other high temperature superconductors, band theory might work in this case. In our work, described below, we find that although electronic structure gives a good description of the structural properties of MgB_2 it is inadequate when it comes to a detailed and quantitative description of the superconducting state properties.

The study of T_c variation with pressure has traditionally been important in the studies on superconducting materials. As T_c depends on the electronic energies, phonon frequencies and the electron–phonon coupling constant,—all of which are fundamental to a proper description of the properties of a superconductor—, the high pressure studies generally focus on these quantities. Recent Raman measurements[10,11] in MgB_2 at high pressure reveal a phonon anomaly near a pressure of 18 GPa. Further, reduction in the T_c variation with pressure, which is believed to be a direct consequence of the hardening of the E_{2g} phonon mode, was also observed near 18 GPa. For further verification, the resistance measurements[12] were carried out in our laboratory, which show an anomaly around the same pressure, thus corroborating the observed phonon anomaly.

As is well known, first principles calculations have contributed significantly in explaining many important phenomena, including resolving controversies, and designing novel materials with tailored physical properties. With application of pressure, the interplay between experiments and first principles calculations has significantly contributed to improvements of techniques in both of them[13]. In fact, though superconductivity in MgB_2 itself was not predicted *a priori*, the *ab initio* calculations have shown[14] as to why its T_c falls at high Al doping concentration. It is concluded that the σ-band electron coupling to E_{2g} mode phonons dictates T_c. These calculations have also shown that different anharmonic terms have significant contributions to E_{2g} mode phonon frequencies[15]. We present here the first principles calculations on electronic states and zone centre phonon frequencies (relevant to the Raman data) of MgB_2 at normal and high pressures, in an effort to understand the observed anomaly, mentioned above, in more detail. We also focus on the frozen-in E_{2g} phonon mode displacement effect on the electronic structure, which indicates the phonon assisted Electronic Topological Transition (ETT)[16] as a possible origin of the high pressure anomaly. Our detailed normal and high pressure first principles calculations for the understanding of the complicated nature of the simple compound MgB_2 points out to some extent, the limitations of the current *ab initio* methods, even at ambient pressure. Further, the high pressure effects, like variation of anharmonic and nonlinear terms under compression, provide further stringent tests of the contemporary theoretical methods. The discrepancies of the quantities predicted by these calculations with the experimental data provide new avenues for further theoretical and computational developments, and improve their predictive powers.

The discovery of high temperature superconductivity in MgB_2 has revived the paradigm of making compounds with light elements as a possible route to high supercon-

*Dedicated to Prof. S. Ramaseshan on his 80th birthday.

†For correspondence. (e-mail: bkgodwal@magnum.barc.ernet.in)

ducting transition temperatures. In spite of some limitations of the first principles calculations in obtaining quantitative agreements with measured properties in the compounds belonging to MgB_2 family, predictions are still feasible by considering some key quantities like density of states at Fermi level etc.[17,18]. Some proposals made in this context are alkali-doped[18] MgB_2 and hole-doped[19] Li-deficient $Li_{0.5}$ BC. In the former case it has not been possible to make the compounds whereas in the latter case, the material is not even metallic[20], presumably due to disorder induced in the doping process. As an alternative effort in this regard, we have considered hole-doped MgB_2C_2 as a designer material for achieving high temperature superconductivity by carrying out the required *ab initio* electronic structure calculations for our prediction. Our results are interesting because this material is expected to be structurally more stable in the doping process than LiBC as the hole doping in it is by replacing the Mg atoms by some other monovalent atoms, in contrast to creating vacancies at the Li sites in LiBC.

We first describe below, the *ab initio* electronic structure studies on MgB_2 at ambient pressure, and the estimates of its properties related to superconductivity, and point out the quantitative disagreements with the measured values to clarify the complexity in the nature of its superconductivity. We then describe our work on MgB_2C_2 to emphasize its claim as a high temperature superconductor. Further, we discuss our high pressure electronic structure calculations with demonstration of phonon-assisted ETT, for the first time, as the probable cause of anomalies observed in the high pressure Raman and transport data. *Ab initio* phonon calculations on MgB_2 at high pressures show the importance of anharmonic and nonlinear terms for estimating some of the phonon frequencies.

Our *ab initio* electronic structure calculations[21] use the Full Potential Linear Augmented Plane Wave (FPLAPW) method as implemented in the WIEN2K code[22]. In our methods we do not use the shape approximation for the potential as both spherical and non-spherical components of the potential have been taken into account in obtaining the radial solutions of the Schrödinger equation inside the muffin-tin spheres. The exchange-correlation terms in the Kohn–Sham equation have been treated within the GGA[23].

We calculate and minimize the total energy with respect to the c/a ratio as well as the volume. Here a and c are the lattice parameters of MgB_2 which crystallizes in the hexagonal (AlB_2) structure. We obtain the equilibrium volume to be 194.08 a.u. with a c/a ratio of 1.151 as compared to the experimental values[1] of 196.04 a.u. and 1.142 respectively. We have fitted the calculated total energies as a function of volume to a smooth function whose derivatives we take to obtain pressure. The bulk modulus B is found to be 148 GPa and compares well with the measured[24,25] value of 152 GPa found from high pressure X-ray diffraction studies. The bulk modulus value estimated by us is used to determine the sound velocity c_s, which in turn enables us to obtain the Debye temperature θ_D. We find θ_D = 733 K whereas the experimental values[2,26] mentioned for θ_D are 750 K and 1050 K. The discrepancies in our values for the bulk modulus and θ_D can be attributed to two reasons. First, we assume an isotropic model for the phonons whereas the hexagonal lattice of MgB_2 is highly anisotropic. Also renormalization of the bulk modulus and sound velocity due to electron–phonon interactions as well as phonon anharmonicities would tend to change these numbers. We thus find that the structural properties of MgB_2 are described reasonably well by the electronic band structure.

The electronic band structure calculated by us is in general agreement with that obtained by other workers[14,27] and shows that the bands near the Fermi energy are predominantly due to boron orbitals. There are four bands which cross the Fermi level, thus giving rise to a multi-sheeted Fermi surface for this compound. The bands are plotted in Figure 1. Two of the bands arise from the π-bonding and antibonding combinations of the B–p_z orbitals whereas the other two bands have their origin from the σ-bonding combinations of the B–sp^2 hybrid orbitals. It is seen from Figure 1 that the σ-bands are degenerate and nearly flat along Γ–A direction. These flat bands largely contribute to the density of states near the Fermi level, thus making a high transition temperature possible.

We now describe our estimation of the superconducting transition temperature T_c. The calculated density of states at the Fermi level $N(E_F)$ enables us to calculate the bare electronic specific heat coefficient γ using the relation $\gamma_{cal} = (1/3)\pi^2 N(E_F) k_B^2$, which is found to be 1.7 mJ/mole-K^2. The estimates made of γ_{exp} from specific heat measurements[2,26] vary from 2.6 mJ/mole-K^2 to 3 mJ/mole-K^2. Thus the mass enhancement factor (1 + λ), where λ is the dimensionless electron–phonon coupling constant, is deter-

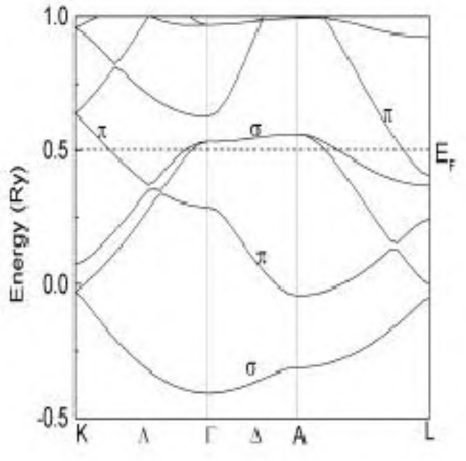

Figure 1. Band structure of MgB_2 at ambient pressure along some high symmetry directions. E_F denotes the Fermi level.

mined using the relation $(1 + \lambda) = \gamma_{exp}/\gamma_{cal}$. This yields the values $\lambda = 0.53$ and $\lambda = 0.77$ corresponding to the two values of γ quoted above. We estimate T_c using the McMillan formula

$$T_c = (\theta_D/1.45)\exp\{-1.04(1 + \lambda)/(\lambda-\mu^*(1 + 0.62\lambda))\}. \quad (1)$$

Here θ_D is the Debye temperature which is determined from lattice specific heat measurements. μ^* is the Coulomb pseudopotential whose value is chosen to be 0.1 as is conventional for *s* and *p* band superconductors. Thus the choice $\lambda = 0.53$ and $\theta_D = 750$ K yields $T_c = 9.4$ K. On the other hand choosing the most favourable parameters ($\lambda = 0.77$ and $\theta_D = 1050$ K) we obtain T_c to be 37 K. In fact assuming the value of μ^*, which is a poorly known quantity, to be 0.093 leads to a T_c of 39 K in this case. The related compound AlB_2 has in comparison one extra electron per formula unit due to the replacement of divalent Mg by trivalent Al. Within a rigid band picture, this is expected to move the Fermi energy away from the flat band feature, leading to a depletion in the density of states at the Fermi energy. This provides a qualitative explanation of the reduction in T_c seen experimentally[3].

Our calculation of T_c has several limitations. The calculations are performed assuming a single superconducting gap whereas it is quite probable[6,7] that MgB_2 is a true multiband superconductor with different gaps on the σ and π sheets of the Fermi surface. Further, MgB_2 has[28] very strong nonlinear electron–phonon coupling as well as strong phonon anharmonicities, both of which effects go beyond present-day formulations for T_c evaluation, with indications that θ_D in eq. (1) should be replaced by a similar quantity based on the E_{2g}-mode phonon frequency only[29] (which however leads to marginal increase of 10% in T_c). The λ parameter has been calculated from first-principles by some workers[14,27] but their results are similar to ours and yield a T_c of the correct size like in our calculations. However none of these calculations incorporate the effects mentioned above.

The basic length scales which characterize a superconductor are the penetration depth and coherence length. The former is the length scale over which magnetic fields vary whereas the latter is the length scale over which the superconducting order parameter varies. Employing linear response theory (see ref. 21 for details) we find that the current **J** is related to the transverse vector potential **A** by the relation

$$\mathbf{J}_\alpha = -\rho^s_{\alpha\beta}\mathbf{A}_\beta, \quad (2)$$

where a summation over repeated indices is implied and $\rho^s_{\alpha\beta}$ is the superfluid density tensor. The London penetration depth λ_α along the direction α ($\rho^s_{\alpha\beta}$ is found to be a diagonal tensor to a very good approximation) is given by $\lambda_\alpha^{-2} = 4\pi\rho^s_{\alpha\alpha}/c$.

Our calculations are performed at T = 0 K where the paramagnetic contribution to $\rho^s_{\alpha\beta}$ vanishes due to the presence of a gap in the quasiparticle excitation spectrum. $\rho^s_{\alpha\beta}$ is easily evaluated from our previously calculated band energies (see ref. 21 for details). We do the calculation separately for one and two gap situations. In the former case, we assume a uniform gap $\Delta(T = 0) = 5$ meV to have opened up over all four sheets of the Fermi surface whereas in the latter case, following Golubov *et al.*[30], we take the larger gap $\Delta_l(T = 0) = 6.2$ meV to have opened over the σ-sheets and the smaller gap $\Delta_s(T = 0) = 2.7$ meV to have opened over the π-sheets. We find that the zero temperature value of the penetration depth is insensitive to the one or two gap scenarios. We obtain the in-plane penetration depth $\lambda_{ab} \sim 86.12$ Å whereas the *c*-axis penetration depth is given by $\lambda_c \sim 306.42$ Å. These values are smaller by a factor of 10 compared to the measured values[8]. To evaluate the coherence length we make use of the BCS relation for an isotropic superconductor $\xi = h v_F/2\pi\Delta$. We assume this relation to hold locally at each **k**-point on the four Fermi sheets. We therefore calculate the Fermi surface average of $|\nabla_k \varepsilon_n(\mathbf{k})|/\pi\Delta_n$ on each of the four Fermi sheets. The coherence length is then obtained as a weighted sum of the lengths calculated on each sheet with weights $D_n(0)/D_{tot}(0)$. Here $D_n(0)$ is the density of states at the Fermi energy due to the *n*th band and $D_{tot}(0)$ is the total density of states at the Fermi energy. We find that the $T = 0$ K coherence length is different in the one gap and two gap situations. In the case of uniform gap we find $\xi_0 \sim 255$ Å whereas in the presence of two gaps, $\xi_0 \sim 377$ Å. These values of the coherence length are larger by a factor of 4 to 5 from the coherence length extracted from upper critical field measurements[9].

The disagreement between our calculated values of λ and ξ and their measured values indicates the inadequacy of the density functional-based electronic band structure results in evaluating the superconducting state properties of MgB_2. Thus it seems that mass renormalization effects due to the strong electron–phonon coupling, believed to be present in this material, need to be included. Also of importance are impurity effects which tend to increase the value of λ and decrease the value of ξ. Thus our results are highly suggestive that MgB_2 is not a clean superconductor.

The occurrence of high temperature superconductivity in MgB_2 has led to an intense search for other possible compounds with light elements that could exhibit even higher transition temperatures. Early theoretical studies[18] on diborides were based on the replacement of Mg by an alkali atom but all efforts to synthesize such compounds have failed. Another possibility that has been explored[19] is the compound $Li_{0.5}BC$, which has BC-planes similar to B-planes in MgB_2, but experimentally it has not even been possible to metallize hole-doped LiBC because of the disorder induced while doping[20]. As an alternative, we have recently considered[31] hole-doped MgB_2C_2 as a candidate for high temperature superconductivity, which

we expect to be structurally less disordered than doped LiBC. MgB_2C_2 forms in an orthorhombic structure with a unit cell that contains graphite-like, but slightly puckered, B–C layers. There is a charge transfer from the Mg atoms to the B–C layers whose charge counterbalances the Mg^{2+} cations.

Our band structure calculations reveal that the parent compound MgB_2C_2 is a band insulator. The bands near the Fermi energy are plotted in Figure 2. Due to a flat band feature seen along the Γ–Z direction the introduction of holes in MgB_2C_2 gives rise to a pocket of holes with a quasi-two dimensional character and a near cylindrical Fermi surface as in MgB_2. The quasi-two dimensional character of the holes implies that if we ignore the k_z dispersion we have a constant density of states for the doped holes, leading to a large density of states at the Fermi energy even for small hole concentrations.

In our calculations we introduced holes by substituting Mg by Li, Na and K. There are two inequivalent Mg positions in the unit cell of the parent compound and so we substituted the alkali atoms at one of the sites preferentially. For the Na-doped material we have also done the calculations with Virtual Crystal Approximation (VCA)[32]. In the latter case we also carried out the calculation for 10% hole doping. Although hole doping causes a slight rearrangement of the bands, the crucial flat band features along the Γ–Z direction and the R–S direction remain intact. In Figure 3 we plot $N(\varepsilon)$, the total electronic density of states per unit volume per spin in the doped compounds. We find that $N(\varepsilon_F) = 0.0564$/Ry-a.u. for 50% Li doping; 0.07149/Ry-a.u. for 50% Na doping, and 0.0794/Ry-a.u. for 50% K doping as compared[21] to 0.0503/Ry-a.u. in MgB_2. The VCA calculation yields $N(\varepsilon_F) = 0.0570$/Ry-a.u. and $N(\varepsilon_F) = 0.0466$/Ry-a.u. for 50% and 10% Na doping respectively. Thus in all hole-doped variants of MgB_2C_2, $N(\varepsilon_F)$ is comparable to that in MgB_2.

We have also made crude estimates of the transition temperature T_c using approximate estimates of λ based on a comparison of our calculated $N(\varepsilon_F)$ with its value in MgB_2. We estimate $T_c \approx 47$ K for the Li-doped compound, $T_c \approx 69$ K for Na doping ($T_c \approx 48$ K for 50% Na doping in the VCA and $T_c \approx 31$ K for 10% Na doping in the VCA) and $T_c \approx 79$ K for K substitution. It is interesting to notice that for 10% Na doping the Fermi energy lies just below a peak in $N(\varepsilon)$. There is thus a possibility of tuning the doping concentration to obtain an even higher T_c. Alkali-doped MgB_2C_2 might be expected to be a strong candidate for observing superconductivity with a high transition temperature.

One may note here that technically more sound methods like coherent potential approximation or its improvements exist for the electronic structure studies on disordered alloys[32]. But the quasi two-dimensional character of the B–C states near the Fermi level being responsible for superconductivity, and the alkali atom substitution of the sites being in the Mg-plane, with no narrow bands involved, the VCA is expected to be adequate.

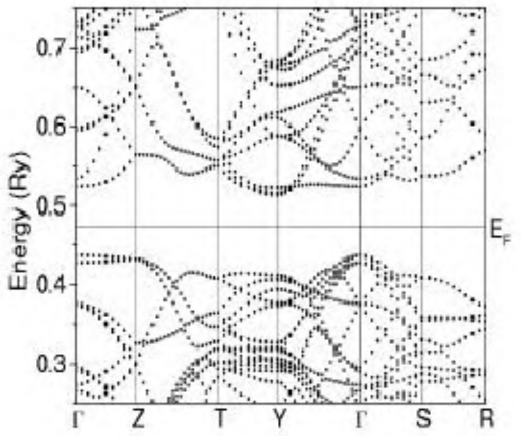

Figure 2. Band structure of MgB_2C_2 along some high symmetry directions at ambient pressure.

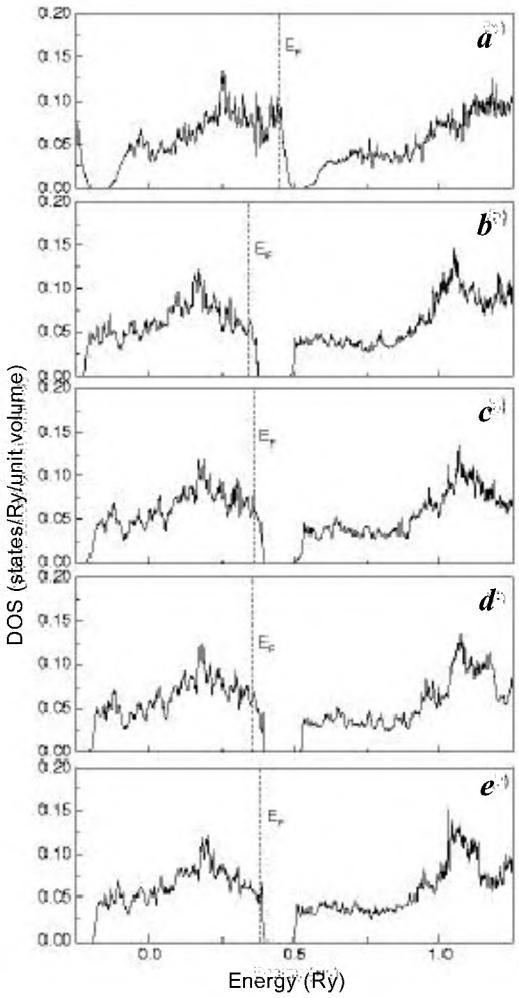

Figure 3. Density of states of (*a*) $Mg_{0.5}K_{0.5}B_2C_2$, (*b*) $Mg_{0.5}Li_{0.5}B_2C_2$, (*c*) $Mg_{0.5}Na_{0.5}B_2C_2$, (*d*) $Mg_{0.5}Na_{0.5}B_2C_2$ in VCA and (*e*) $Mg_{0.9}Na_{0.1}B_2C_2$ in VCA.

As mentioned earlier, Raman measurements[10,11] of the E_{2g} phonon frequency under high pressure have revealed an interesting anomaly near 18 GPa. Early measurements by Meletov *et al.*[10] found that the frequency of the E_{2g} mode increases linearly with pressure. However the slope of the variation changed discontinuously at 5 GPa and again near 18 GPa. The first change was attributed by them to have extrinsic origins whereas the latter anomaly was a genuine effect most probably due to an electronic topological transition, especially as structural transitions were not observed in the X-ray diffraction studies[12,25]. Their results were confirmed by Goncharov and Struzhkin[11] who also observed a phonon anomaly near 18 GPa although they found the variation of the phonon frequency with pressure to be nonlinear. Further, the T_c variation with pressure also showed[11] an anomaly near 18 GPa.

In order to get an independent verification of this anomaly, electrical resistance measurements were carried out as a function of applied pressure by the recently commissioned technique in a diamond anvil cell in our laboratory (see ref. 12 for experimental details). These measurements, while loading as well as unloading, revealed that the resistance decreases continuously with applied pressure up to 18 GPa when it shows a discontinuous fall by almost 33%. Thus the resistance measurements also corroborate the phonon anomaly.

To obtain an understanding of the nature of the anomaly we performed electronic structure calculations of MgB_2 under compression as no high pressure band structure has been reported so far in the literature. We found that although the bands move about a little, there is no ETT for the static high pressure equilibrium positions of atoms. We therefore turned our attention to the possibility of phonon-assisted ETT. To explore this possibility we initially performed the band structure calculation at ambient pressure with a frozen-in displacement corresponding to the E_{2g} phonon mode. The root mean square (r.m.s.) B atom displacement was chosen to be 0.06 Å. There is a splitting of the σ-bands along the Γ–A direction with the lower band intercepting the Fermi level. The band structure is shown in Figure 4. The results are in agreement with those obtained earlier by An and Pickett[14] who took 0.057 Å as the r.m.s. displacement. To approximately estimate the B atom displacement at 18 GPa, we assumed that the energy in each mode is characterized by the temperature, as in harmonic vibration, and use the relation $\Omega_0^2\langle u_0^2\rangle = \Omega_p^2\langle u_p^2\rangle$ where Ω_P is the phonon frequency and u_P the B-atom displacement at a pressure P.

To proceed further we calculated the E_{2g} phonon frequency at the Γ-point using the plane wave self-consistent field (PWSCF) method[33]. At the harmonic level we find a linear variation of the frequency with pressure. Our results for the phonon frequency as a function of pressure are plotted in Figure 5. There is no anomaly seen near 18 GPa. The values of the phonon frequencies too are smaller than those experimentally observed throughout the pressure range considered by us. It is known[28] that anharmonic effects, which are believed to be strong, have the effect of hardening the phonon frequency. Having estimated the phonon frequency we are now in a position to get an r.m.s. value of 0.047 Å for the B-atom displacement at 18 GPa. Using this number we once again calculate the band structure. The obtained band structure is shown in Figure 6. Along the Γ–A direction, the lower split σ-band almost touches the Fermi level. This result is an indication that there is a phonon-assisted ETT at high pressure, around 20 GPa (as this flat band along Γ–A, though split, does not intersect the Fermi level), which is close to the pressure at which anomalies are seen in the variations of E_{2g} mode phonon frequency, resistivity, and T_c. Note however that these first principles results and the nature of ETT are to some extent different from the model suggested by Goncharov and Struzhkin[11].

Thus phonon-assisted ETT is the probable cause of the anomalies seen in the phonon spectrum and the electrical resistance. However to obtain the phonon anomaly in our first principles calculations of the phonon spectrum requires inclusion of anharmonic effects. Anharmonic

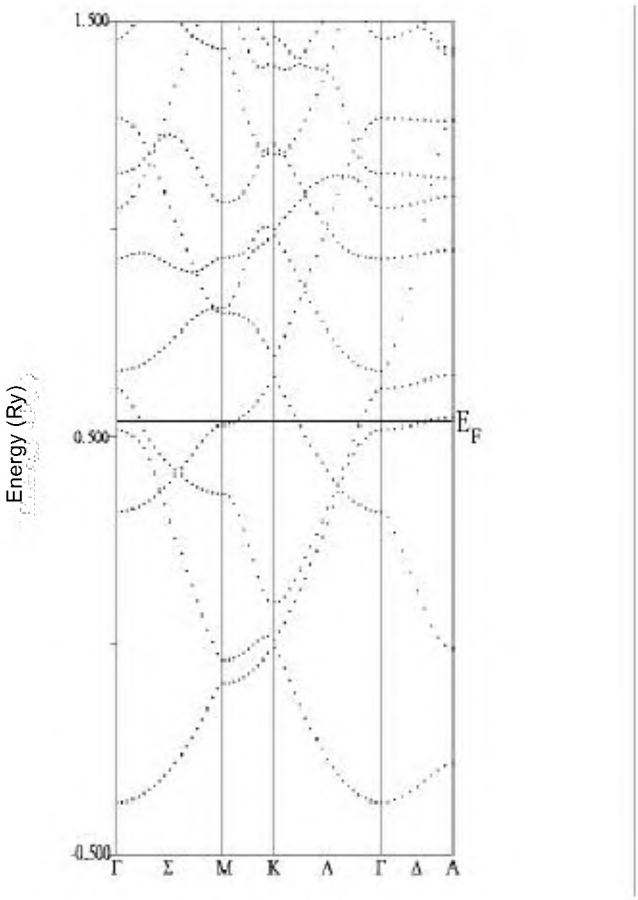

Figure 4. Band structure of MgB_2 with a frozen-in E_{2g} phonon-mode displacement at ambient pressure.

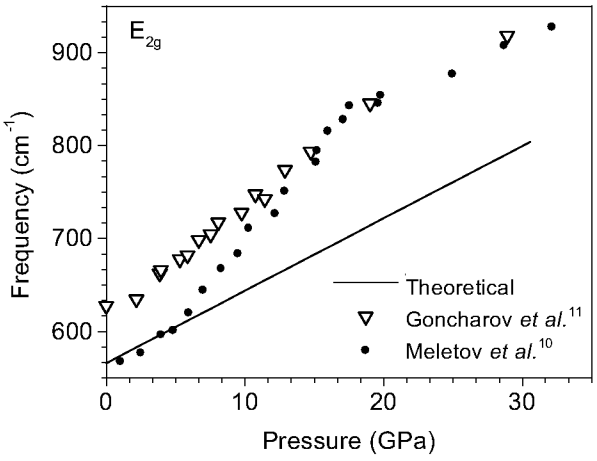

Figure 5. E_{2g} phonon frequency as a function of pressure: theory and experiment (refs 10, 11).

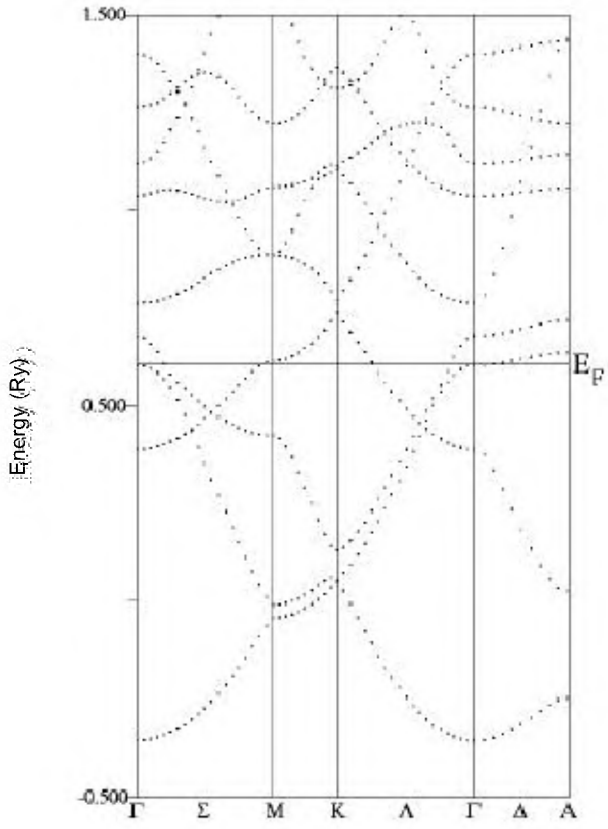

Figure 6. Band structure of MgB_2 with a frozen in E_{2g} phonon displacement at 18 GPa.

corrections to the phonon frequencies in MgB_2 have been reported at ambient pressure[15,28]. These studies indicate that the quartic term is dominant and has the effect of hardening the phonon frequencies. The discrepancy between our calculated harmonic frequencies and the experimental values indicates that the anharmonic effects initially increase with pressure until at high pressures there is a kind of saturation effect, and although the measured phonon frequencies are larger than the theoretical values, both curves are parallel when plotted as a function of pressure (Figure 5). Further, there may be a large contribution to the Raman mode frequency from the strong electron–phonon coupling present in MgB_2, which is difficult to calculate because of the nonlinear nature of the coupling[28]. Improvements in the theoretical techniques to include the second order perturbation terms in the electron orbitals may be necessary for estimating further details of anharmonic and nonlinear terms, and in obtaining the signatures of ETT in the phonon spectra. Note that anomalies due to ETT are less pronounced than those pertinent to the conventional phase transitions, and hence accurate calculations and innovative techniques may be needed to obtain their signatures[34]. Thus anomalies seen in MgB_2 emphasize the significance of high pressure studies in leading to new avenues in the theoretical and computational developments based on the first principles calculations.

In conclusion, MgB_2 is an electron–phonon superconductor. However the presence of strong nonlinear electron–phonon coupling as well as strong anharmonicities in the phonon spectrum make it a difficult job to predict its properties from first-principles theories. The possible presence of two superconducting gaps is an added complication. We have attributed the observed high pressure anomalies in MgB_2 around 18 GPa to phonon-assisted ETT by carrying out, for the first time, the high pressure electronic structure calculations with frozen-in E_{2g} phonon mode displacements of atoms. Our *ab initio* high pressure phonon calculations, based on the density functional perturbation theory, do not show the observed high pressure anomaly near 18 GPa. Thus our high pressure studies point out the need to include anharmonic and/or nonlinear terms in the first principles-based estimates, especially in evaluating effects of relatively less noticeable phenomena like ETT. The occurrence of high temperature superconductivity in MgB_2 holds out hope that other similar materials with light atoms could exhibit high transition temperatures as well, and we have demonstrated, by the electronic structure calculations, that alkali-doped MgB_2C_2 is a prime candidate for this.

1. Nagamatsu, J., Nakagawa, N., Muranaka, T., Zenitani, Y. and Akimitsu, J., *Nature*, 2001, **410**, 63.
2. Bud'ko, S. L., Lapertot, G., Petrovic, C., Cunningham, C. E., Anderson, N. and Canfield, P. C., *Phys. Rev. Lett.*, 2001, **86**, 1877.
3. Slusky, J. *et al.*, *Nature*, 2001, **410**, 343.
4. Karapetrov, G., Javarone, M., Kwok, W. K., Crabtree, G. W. and Hinks, D. G., *Phys. Rev. Lett.*, 2001, **86**, 4374.
5. Takahashi, T., Sato, T., Souma, S., Muranaka, T. and Akimitsu, J., *Phys. Rev. Lett.*, 2001, **86**, 4915.

6. Chen, X. K., Konstantinovic, M. J., Irwin, J. C., Lawrie, D. D. and Franck, J. P., *Phys. Rev. Lett.*, 2001, **87**, 157002.
7. Szabo, P. *et al.*, *Phys. Rev. Lett.*, 2001, **87**, 137005.
8. Niedermayer, Ch. *et al.*, preprint cond-mat/0108431, 2001.
9. de Lima, O. F., Ribeiro, R. A., Avila, M. A., Cardoso, C. A. and Coelho, A. A., *Phys. Rev. Lett.*, 2001, **86**, 5974.
10. Meletov, K. P., Kulakov, M. P., Kolesnikov, N. N., Arvanitidis, J. and Kourouklis, G. A., *JETP Lett.*, 2002, **75**, 406.
11. Goncharov, A. F. and Struzhkin, V. V., *Physica*, 2003, **C385**, 117.
12. Garg, A. B., Vijayakumar, V. and Godwal, B. K. (to be published).
13. Godwal, B. K., In *Advances in High Pressure Science and Technology* (ed. Singh, A. K.), Tata McGraw-Hill, New Delhi, 1995, p. 23.
14. An, J. M. and Pickett, W. E., *Phys. Rev. Lett.*, 2001, **86**, 4366.
15. Lazzeri, M., Calandra, M. and Mauri, F., preprint cond-mat/0306650.
16. Lifshitz, I. M., *Zh. Eksp. Teor. Fiz.*, 1960, **38**, 1569; [*Sov. Phys. JETP*, 1960, **11**, 1130].
17. Ravindran, P., Vajeeston, P., Vidya, R., Kjekshus, A. and Fjellvåg, H., *Phys. Rev.*, 2001, **B64**, 224509.
18. Singh, P. P., *Phys. Rev. Lett.*, 2001, **87**, 087004.
19. Rosner, H., Kitaigorodsky, A. and Pickett, W. E., *Phys. Rev. Lett.*, 2002, **88**, 127001.
20. Bharati, A. *et al.*, preprint cond-mat/0207448.
21. Gaitonde, D. M., Modak, P., Rao, R. S. and Godwal, B. K., *Bull. Mater. Sci.*, 2003, **26**, 137.
22. Blaha, P. *et. al.*, *Comp. Phys. Commun.*, 1990, **59**, 399; Blaha, P. *et al.*, 2001, WIEN2k (An APW+ local orbital program for calculating crystal properties, Techn. Universitat, Wien, Austria).
23. Perdew, J. P., Burke, K. and Ernzerhof, M., *Phys. Rev. Lett.*, 1996, **77**, 3865.
24. Vogt, T. *et al.*, preprint cond-mat/0102480, 2001.
25. Garg, A. B., Vijayakumar, V. and Godwal, B. K., 2001 (unpublished).
26. Bouquet, F. *et al.*, *Phys. Rev. Lett.*, 2001, **87**, 047001.
27. Kortus, J., Mazin, I. I., Belashchenko, K. D., Antropov, V. P. and Boyer, L. L., *Phys. Rev. Lett.*, 2001, **86**, 4656.
28. Yildirim, T. *et al.*, *Phys. Rev. Lett.*, 2001, **87**, 037001.
29. Canfield, P. C. and Crabtree, G. W., *Phys. Today*, 2003, **56**, 34.
30. Golubov, A. A. *et al.*, *J. Phys. Cond. Matt.*, 2002, **14**, 1353.
31. Verma, A. K., Modak, P., Gaitonde, D. M., Rao, R. S., Godwal, B. K. and Gupta, L. C., *Europhys. Lett.*, 2003, **63**, 743.
32. Ehrenreich, H. and Schwartz, L. M., In *Solid State Physics* (eds Ehrenreich, H., Seitz, F. and Turnbull, D.), Academic, New York, 1976, vol. 31.
33. Baroni, S., de Gironcoli, S., Corso, A. D. and Giannozzi, P., *Rev. Mod. Phys.*, 2001, **73**, 515.
34. Godwal, B. K., Meenakshi, S., Modak, P., Rao, R. S., Sikka, S. K., Vijayakumar, V., Bussetto, E. and Lausi, A., *Phys. Rev.*, 2002, **B65**, 140101.

Received 4 September 2003

High pressure studies on a nematogen with highly polar molecules: Evidence for a nematic–nematic transition*

V. Manjuladevi and N. V. Madhusudana†
Raman Research Institute, C.V. Raman Avenue, Bangalore 560 080, India

We have modified a high pressure optical set-up to enable measurements on the optical path difference of aligned liquid crystals. We present the phase diagram of a polar nematogen, viz. *p*-cyanophenyl *p-n* heptylbenzoate which is shown to exhibit a nematic (N_d) to nematic (N_1) transition in the bulk at elevated pressures. We have also measured the temperature variations of the orientational order parameter (S) at various pressures to find that S has constant values at both the nematic to isotropic and N_d to N_1 transitions at different pressures.

LIQUID crystals (LCs) made of rod-like molecules with polar end groups exhibit interesting phase sequences like smectic polymorphism, the reentrant nematic phase double reentrance, etc.[1,2]. Both phenomenological and molecular theoretical models have been developed to explain these phenomena[1]. In uniaxial nematics (N), the long axes of the molecules are oriented on the average about the director $\hat{n}$, which is a dimensionless apolar unit vector. The apolar nature of the director in nematogens with highly polar end groups can be understood, as the molecules have an anti-parallel short-range order in the medium[3]. Smectic A (SmA) LCs have a layering order, with the layer normal ($\hat{z}$) being parallel to $\hat{n}$. In polar compounds which exhibit reentrant N and SmA phases, the high temperature smectic A_d (SmA_d) phase has partial bilayer order with $l < d < 2\,l$, where l is the molecular length, and d the layer spacing. The low temperature smectic A_1 (SmA_1) phase has a layer spacing equal to the monomolecular length, i.e. $d = l$. The unusual phenomena exhibited by highly polar compounds have been successfully explained by Prost and co-workers using a phenomenological Landau theory. This model[1] takes into account the coupling between two smectic order parameters corresponding to the two lengths mentioned above. One of the consequences of this model is the prediction of an N_d to N_1 transition line in continuation of the SmA_d to SmA_1 transition line, the latter being characterized by an appropriate jump in the layer spacing. Indeed, such an N–N transition has been found as a continuation of the SmA_1–SmA_d transition line in the concentration–temperature phase diagram of a binary mixture of polar

*Dedicated to Prof. S. Ramaseshan on his 80th birthday.
†For correspondence. (e-mail: nvmadhu@rri.res.in)